Estuarine, Coastal and Shelf Science 173 (2016) A1–A15

Contents lists available at ScienceDirect

Estuarine, Coastal and Shelf Science

journal homepage: www.elsevier.com/locate/ecss

Invited feature

Changes in water clarity in response to river discharges on the Great Barrier Reef continental shelf: 2002–2013

K.E. Fabricius [a, *], M. Logan [a], S.J. Weeks [b], S.E. Lewis [c], J. Brodie [c]

[a] Australian Institute of Marine Science, PMB No 3, Townsville, Queensland 4810, Australia
[b] Biophysical Oceanography Group, School of Geography, Planning and Environmental Management, University of Queensland, Brisbane 4072, Australia
[c] Centre for Tropical Water & Aquatic Ecosystem Research, James Cook University, Townsville, Queensland, 4811, Australia

ARTICLE INFO

Article history:
Received 31 May 2015
Received in revised form
19 February 2016
Accepted 2 March 2016
Available online 10 March 2016

Regional index terms:
Australia
Queensland
Great Barrier Reef (10.5°–24.0° latitude South, 142.5°–153.5° longitude East)

Keywords:
Turbidity
Water clarity
Photic depth
Continental shelf seas
Tropical coral reefs
Crown-of-thorns starfish

ABSTRACT

Water clarity is a key factor for the health of marine ecosystems. The Australian Great Barrier Reef (GBR) is located on a continental shelf, with >35 major seasonal rivers discharging into this 344,000 km^2 tropical to subtropical ecosystem. This work investigates how river discharges affect water clarity in different zones along and across the GBR. For each day over 11 years (2002–2013) we calculated 'photic depth' as a proxy measure of water clarity (calibrated to be equivalent to Secchi depth), for each 1 km^2 pixel from MODIS-Aqua remote sensing data. Long-term and seasonal changes in photic depth were related to the daily discharge volumes of the nearest rivers, after statistically removing the effects of waves and tides on photic depth. The relationships between photic depths and rivers differed across and along the GBR. They typically declined from the coastal to offshore zones, and were strongest in proximity to rivers in agriculturally modified catchments. In most southern inner zones, photic depth declined consistently throughout the 11-year observation period; such long-term trend was not observed offshore nor in the northern regions. Averaged across the GBR, photic depths declined to 47% of local maximum values soon after the onset of river floods, and recovery to 95% of maximum values took on average 6 months (range: 150–260 days). The river effects were strongest at latitude 14.5°–19.0°S, where river loads are high and the continental shelf is narrow. Here, even offshore zones showed a >40% seasonal decline in photic depth, and 17–24% reductions in annual mean photic depth in years with large river nutrients and sediment loads. Our methodology is based on freely available data and tools and may be applied to other shelf systems, providing valuable insights in support of ecosystem management.

1. Introduction

The ecology of marine ecosystems is strongly governed by water clarity (turbidity, or transparency). Reduced water clarity leads to a significant loss in light, affecting photosynthetic organisms such as corals and seagrasses (Anthony and Hoegh-Guldberg, 2003; Collier et al., 2012). Chronically low water clarity limits the depth distribution of seagrasses and coral reefs to shallow waters, with a daily average of 4–8 mol photons m^{-2} day^{-1} (~6–8% of surface irradiance) considered to be a typical minimum light requirement for ecosystem maintenance (Gattuso et al., 2006). Reduced water clarity is also often related to increasing concentrations of suspended particles and their associated nutrients, which benefit filter- and deposit-feeding animals. In coral reefs, the nutrients associated with reduced water clarity can therefore lead to shifts from corals to macroalgae, and at more severe conditions, macroalgae are replaced by heterotrophic filter feeders (Birkeland, 1988; De'ath and Fabricius, 2010). Water clarity can even affect coral reef fishes, including their larval settlement, gill structures, and predator-prey interactions (Wenger et al., 2011, 2013; Hess et al., 2015).

The main factors causing short-term episodic losses in water clarity in shallow shelf seas are well understood. They include the depth-dependent resuspension of seafloor sediments by waves and tides, and turbid river plumes (Larcombe et al., 1995; Wolanski et al., 2005; Piniak and Storlazzi, 2008; Storlazzi and Jaffe, 2008; Storlazzi et al., 2009). However, chronic changes in water clarity, and their links to recently-delivered terrigenous sediments and nutrients are less understood. This is especially true in shelf seas, in which vast areas of seafloor are covered by sediments, the majority

* Corresponding author.
E-mail address: k.fabricius@aims.gov.au (K.E. Fabricius).

http://dx.doi.org/10.1016/j.ecss.2016.03.001

of which are historic deposits and typically only small proportions are recently imported.

For the Great Barrier Reef (GBR) in north-eastern Australia, the topic of changes in water clarity is the subject of contention (e.g. Orpin and Ridd, 2012; Fabricius et al., 2014; Lewis et al., 2014b). The GBR is located on a shallow continental shelf, and with an area of 344,000 km^2 is one of the largest World Heritage Areas on Earth. Understanding what controls water clarity in this huge area is important, as the GBR houses important ecosystems, comprising >3000 individual coral reefs, extensive seagrass meadows and other diverse inter-reefal habitat types. In recent decades, the GBR has received an annual average of ~17 million tonnes of terrigenous sediments, 80,000 tonnes of nitrogen, and 16,000 tonnes of phosphorus from its 35 river basins. These nutrient and sediment discharges are ~2–8-fold higher than estimated loads pre-dating European settlement in the mid-19th century (Kroon et al., 2012; Waters et al., 2014).

The question as to whether or not these additional river nutrient and sediment loads affect water clarity and ecosystem health is subject to ongoing scientific debate, and is also a significant concern for management agencies. Some researchers have suggested that the effect of newly delivered riverine materials on water clarity is negligible, arguing that the historically deposited sediments on the inshore 'sediment wedge' dominate resuspension regimes (Larcombe et al., 1995; Orpin and Ridd, 2012). In contrast, other studies have proposed that newly delivered materials are of different composition (e.g., organically enriched) and more readily resuspended compared to historic seafloor sediments (Fabricius et al., 2013, 2014; Lewis et al., 2014b; van Maren et al., 2014; Seers and Shears, 2015). Considerable government investments have been made in order to reduce the high river loads of nutrients and sediments (State of Queensland, (2013)). If the spatial and/or temporal extent of river effects on water clarity differed among regions and were known, then these investments could be more effectively targeted. If, however, water clarity was not linked to the inputs of newly delivered materials but was rather determined by resuspension of existing sedimentary deposits, then the ecological benefits of such investment may be marginal.

GBR river plumes and resulting water quality conditions are governed by the shallow shelf sea, complex hydrodynamics, and the large spatial scale of the GBR spanning over 12° latitude (Fig. 1). Rainfall is episodic and highly seasonal, and rivers discharge into the GBR for only a few weeks during the summer wet seasons. River plumes are typically relatively short-lived and are detectable within ~20 km of the coast, although large plumes can travel hundreds of kilometres longshore (mostly north) and also offshore, depending on wind and current regimes (Brodie et al., 2010; Alvarez-Romero et al., 2013). Extended flood plumes are dominated by suspended sediment near the river mouth, by sediment flocs in the mid-section of the plume, and by phytoplankton in their furthest reaches (Bainbridge et al., 2012; Devlin et al., 2012). This zonation is due to coarser sediments (>16 μm) settling out near the river mouth (Bainbridge et al., 2012), whereas the finer nutrient-rich fraction is transported further away by currents until flocculation facilitates its settlement, and phytoplankton successions take some days to develop in response to the river nutrients and improving light.

The settled fine sediments, particularly those in the <16 μm particle size class, are important carriers of particulate nutrients, and in combination with dissolved nutrients they foster the production of particulate organic matter and organic-rich flocs that are easily resuspendible whilst in shallow waters (Bainbridge et al., 2012). In addition, certain clay minerals are carried over long distances in the plumes due to properties such as cation exchange capacity, particle size, and charge density (Hillier, 1995; Douglas et al., 2006), contributing to floc formation (Bainbridge et al., 2012). This sediment fraction is easily resuspended due to its low density. Indeed, it is this fine, organic-rich sediment that has a strong influence on light attenuation in the marine environment (Storlazzi et al., 2015). Repeated iterations of resuspension and deposition gradually shift the newly imported material offshore beyond the depth of resuspension, or into wave-sheltered bays (Orpin et al., 2004; Wolanski et al., 2008; Bainbridge et al., 2012; Lewis et al., 2014b). Nepheloid flows and tropical cyclones also contribute to the transport of coastal sediments into deeper offshore waters (Wolanski et al., 2003).

Remote sensing data provide daily estimates of water clarity conditions, and are suitable for the investigation of spatial and temporal variation in marine water clarity. For example, a study based on 8 years of remote sensing data showed that seasonal variability in Secchi depth in Florida's Tampa Bay was mainly due to chlorophyll concentrations controlled by river runoff in the rainy season and sediment resuspension in the dry season (Chen et al., 2007b). Drivers of turbidity also differed across sub-regions in this bay, being dominated by wind-driven resuspension in the lower reaches, and by river sediments in the upper portion of the Bay (Chen et al., 2007a). For the Florida Keys, remote sensing data were used to demonstrate how water clarity increases with distance from the shore, from north to south, and changes seasonally due to current reversals driven by shifting prevailing winds (Barnes et al., 2013). Extreme weather events can also drive variation in water clarity, as documented for Florida (Sheridan et al., 2013), New Zealand (Seers and Shears, 2015) and the French Bay of Biscay (Petus et al., 2014b). Remote sensing data are especially useful for assessing changes in water clarity and their drivers, in areas that are as large, complex, and ecologically and economically valuable as the GBR.

In this study we use remote sensing data, collected daily over 11 years, together with daily and annual data on environmental drivers, to investigate (1) long-term trends in daily water clarity, and differences in the strength of association and lag times between daily water clarity and river discharges, in relation to proximity to river and catchment modification across and along the GBR; (2) seasonal trends in daily water clarity, and their relationships to daily river discharges; and (3) rates of change of photic depth between years with high and low river nutrient and sediment loads in the different zones. We determine the areas at greatest risk of loss in water clarity from river discharges, demonstrate for how long how water clarity was diminished throughout the year, and measure the rates of recovery for each of the zones. We present a sequence of advanced statistical methods that was optimised to deal with such large and complex data. Our methodology is based on freely available data and statistical tools, and is transferrable to other parts of the world and other drivers. Its application could lead to a better understanding of processes determining marine water clarity in coastal seas.

2. Methods

2.1. Study region

GBR catchments vary greatly in their level of human use. The remote far northern Cape York has limited agricultural and no urban development, whereas the Wet Tropic and Whitsunday regions have high proportions of land used for fertilised cropping (particularly sugarcane cultivation) (Fig. 1, Supplementary Table S1). The Burdekin and Fitzroy regions are large catchments (>30,000 km^2) with land use dominated by rangeland cattle grazing, and although fertilised cropping (sugarcane and grains) comprises a small percentage of their total catchment area, cropping lands do occupy

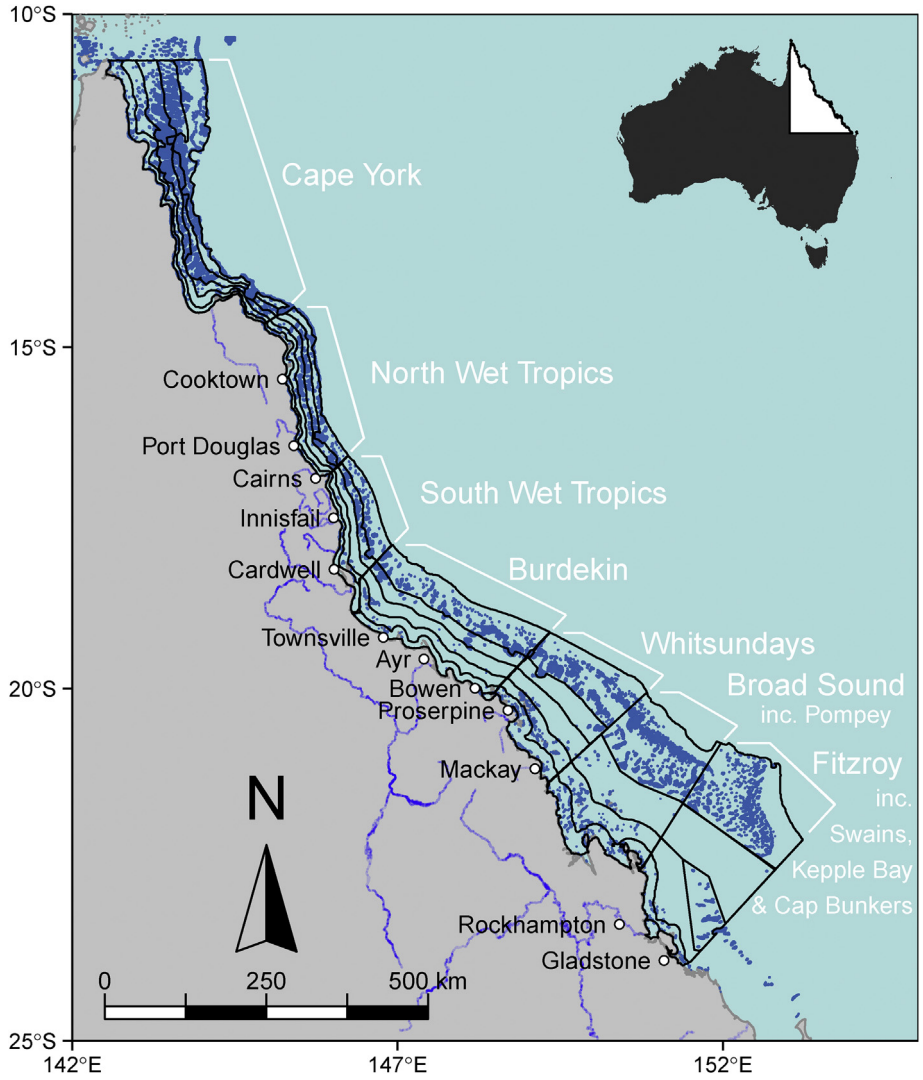

Fig. 1. Map of the 2000 km long Great Barrier Reef, showing the boundaries of the 35 zones in the seven GBR regions. The regions are (from north to south): Cape York, Northern and Southern Wet Tropics, Burdekin, Whitsunday, Broad Sound with the Pompey reefs, and Fitzroy with Keppel Bay, Capricorn Bunker group and the Swain reefs. The main rivers are mapped as blue lines.

large areas in absolute terms. Urban populations are low throughout the GBR Catchment, with the total population being ~1 million people. The majority of this population is concentrated in 6 small cities (70,000–200,000 persons) along the >2000 km long coastline (Supplementary Table S1) (Brodie and Waterhouse, 2012; Waters et al., 2014).

To facilitate regional and cross-shelf comparisons, the GBR data were spatially aggregated into seven geographic regions (Fig. 1, Table 1). The northern GBR was subdivided into three long-shore regions, with the '*Cape York*' Region extending from 10.5° to14.5° latitude South (the northern edge of the GBR to Lizard Island), and the '*Northern Wet Tropic*' and '*Southern Wet Tropic*' Regions extending to ~17° and ~18.3° South, respectively. These delineations best capture differences in geomorphology, rainfall, and agricultural use patterns (Table 1, Supplementary Table S1), and population outbreak dynamics of the coral-eating crown-of-thorns starfish (Fabricius et al., 2010). In the central GBR, the boundaries of the *Burdekin* Region followed the earlier analysis of Fabricius et al. (2014). The southern GBR was divided into three long-shore regions, as the *Broad Sound* Region with its high tidal range and distance from major rivers is unrepresentative of the more intensely used and populated *Whitsunday* and *Fitzroy* Regions.

To assess how the river effects extended across the continental shelf into offshore waters, each of the seven regions was further subdivided into zones parallel to the coast. Five zones were defined in most regions, based on the percentage of total distance across the continental shelf: *Coastal:* 0–10%, *Inshore:* 10–25%, *Lagoon:* 25–45%, *Midshelf:* 45–0.65%, and *Outershelf:* 65–100%. The Fitzroy Region was partitioned by combinations of oceanographic and geomorphological characteristics, to account for geographic complexities around the Capricorn-Bunker and Swain Reefs, and the estuarine Keppel Bay. The cross-shelf zone boundaries of the Broad Sound were chosen to best match those of both the Whitsunday and Fitzroy areas. Regions were categorised into groups of low and high modification (Cape York and Broad Sound, *vs.* the rest). Zones were also broadly classified as close and far from river influences, depending on the width of the continental shelf, hydrodynamics and river sizes (Supplementary Table S2). A more refined grouping was not possible due to the greatly varying river sizes, the large sizes of the zones with one or several rivers entering into each zone, and the complex hydrodynamics in the GBR.

Table 1
The major rivers included in the models for each of the study regions and zones, based on the location of their river mouth, and assuming predominant northerly current direction. Also shown are the estimated cumulative end-of-river estimates of freshwater discharges, and loads of particulate phosphorus (PP) and total suspended sSolids (TSS), summed across the water years 2002–2013 (from Lewis et al., 2014a).

Region/Zone	Rivers	River freshwater volumes (10^6 ML)	River PP loads (tonnes)	River TSS loads (10^6 tonnes)
Cape York (all zones)	Normanby, Endeavour, Stewart	84[a]	1,400[a]	3.1[a]
Northern Wet Tropic (all zones)	Daintree, Barron, Russell, Mulgrave, North and South Johnstone; Burdekin (30% of discharge)	195	32,800	24
Southern Wet Tropic (all zones)	Russell, Mulgrave, North and South Johnstone, Tully, Herbert; Burdekin (50% of discharge)	286	42,800	42
Burdekin (all zones)	Burdekin	152	23,600	51
Whitsundays (all zones)	Proserpine, O'Connell, Pioneer	47	4,700	4.9
Broad Sound -Pompey (all zones), Keppel Bay	Fitzroy River	85	24,200	22
Fitzroy-Swain (all zones except Keppel Bay)	Fitzroy, Burnett	85	24,200[b]	22[b]

[a] No data for Endeavour, Stewart Rivers.
[b] No data for Burnett River.

2.2. Remote sensing data

To quantify water clarity from remote sensing data, 1 km^2 Moderate Resolution Imaging Spectroradiometer (MODIS-Aqua) data were processed for 'photic depth' (Z%; unit: m), as an equivalent to Secchi depth Weeks et al., 2012). This GBR-specific algorithm of photic depth was derived from ~5000 comparisons of GBR *in situ* Secchi depth observations and MODIS and Sea-viewing Wide Field-of-view Sensor (SeaWiFS) observations, following Lee et al. (2007). Amongst the current algorithms to derive the multispectral diffuse attenuation coefficient (K_d) from satellite data, the quasi-analytical algorithm by Lee et al. (2005, 2007) was found to perform best in coastal and shallow waters such as the GBR (Weeks et al., 2012) and southern Florida (Barnes et al. (2013, Zhao et al., 2013). In optically complex waters, such correlation-based algorithms typically provide better results than traditional algorithms based on the diffuse attenuation coefficient of the downwelling spectral irradiance, either at 488 nm wavelength (K_{d488}) or of all photosynthetically available radiation (K_{dPAR}) (IOCCG, 2006; Saulquin et al., 2013). Spatial masks were used to extract data from the area between the coast and 200 m isobath, and to exclude optically contaminated pixels (reefs and very shallow coastal seafloor). The daily data were processed for all 153,177 grid points from 1st July 2002 to 30 September 2013, pixels with cloud contamination were removed, and data were aggregated into the 35 zones across seven geographic regions (Fig. 1, Table 1).

2.3. Wave, wind and tidal data

Short-term fluctuations in water clarity in shallow shelf seas are strongly co-determined by wind waves and the tidal resuspension of seafloor sediments (Fabricius et al., 2014), and hence the effects of these covariates were statistically removed in the analyses for each zone and day (Fig. 2). To do so, data on wave heights and frequencies were obtained from the Queensland State Government, Department of Environment and Heritage Protection, based on the four coastal wave rider buoys available in the GBR (Supplementary Fig. S1). Although the data underestimate wave height for the offshore zones, they have high predictive power of differences in photic depth between rough and calm days. For Cape York (latitude 10.5°–14.5° S), no wave data were available. Instead wind data from Lockhart River (12.47°S) were obtained from the Bureau of Meteorology (http://www.bom.gov.au/climate/how/newproducts/IDCdw.shtml). The hourly wave and wind data were averaged to daily values.

Predicted daily tidal amplitudes were used as a proxy for tidal currents and were estimated from a harmonic tidal clock (xtide; Flatter, 2005) using the 2004-06-14 harmonics parameters (https://github.com/manimaul/MX-Tides-iOS/blob/master/resources/harmonics-2004-06-14.tcd). Representative tidal locations were chosen, and the maximum daily tidal amplitude was calculated for each zone and day (Supplementary Fig. S1, Table S2).

2.4. River data

To assess the links of changes in photic depths in the GBR to river discharges, the main influential rivers were identified for each region (Devlin et al., 2015), based on the prevailing predominantly northerly currents along the shore. The main rivers in the Burdekin, Whitsunday and Fitzroy Regions are relatively unambiguous (Fig. 1, Table 1). The Southern and Northern Wet Tropics have many rivers directly discharging into the regions, and are additionally affected by rivers from further south (Alvarez-Romero et al., 2013). For the Northern Wet Tropics Region, the total daily discharge values were calculated as the sum of the discharge from the Daintree, Barron, Russell-Mulgrave and Johnstone (North and South) Rivers, plus 30% of the freshwater volumes of the very large but distant (>350 km) Burdekin River as a best approximation of flood dispersal estimates based on hydrodynamic models and remote sensing imagery (Alvarez-Romero et al., 2013; Brinkman et al., 2014). For the Southern Wet Tropics Region, the total daily discharge values were calculated as the sum of the Russell-Mulgrave, Johnstone, Tully and Herbert Rivers, and 50% of the Burdekin River volumes. For the Broad Sound Region with its high tidal range and the absence of major rivers, only the large Fitzroy River was considered to be of influence. The multiple small streams of the Plane Basin may have additional influence but are not gauged.

River data for all of the northern half of the remote Cape York Region were not available since there are only gauging stations in the small southern Stewart and Endeavour Rivers, and in the large Normanby Rivers since 2005. As an alternative to river discharge data, we used daily rainfall data from the Lockhart River rainfall gauge (Australian Bureau of Meteorology, http://www.bom.gov.au/oceanography/projects/abslmp/data/index.shtml), which provided daily records throughout the observation period.

Two sets of river data were used (Fig. 2). The first set constituted of daily data of discharge volumes, measured at gauging stations and provided by the State of Queensland, Department of Natural Resources and Mines. Many gauging stations are located inland from the river mouth and hence under-estimate daily freshwater discharge volumes at the river mouth, but their relative discharge estimates are useful proxies for temporal patterns in river flows.

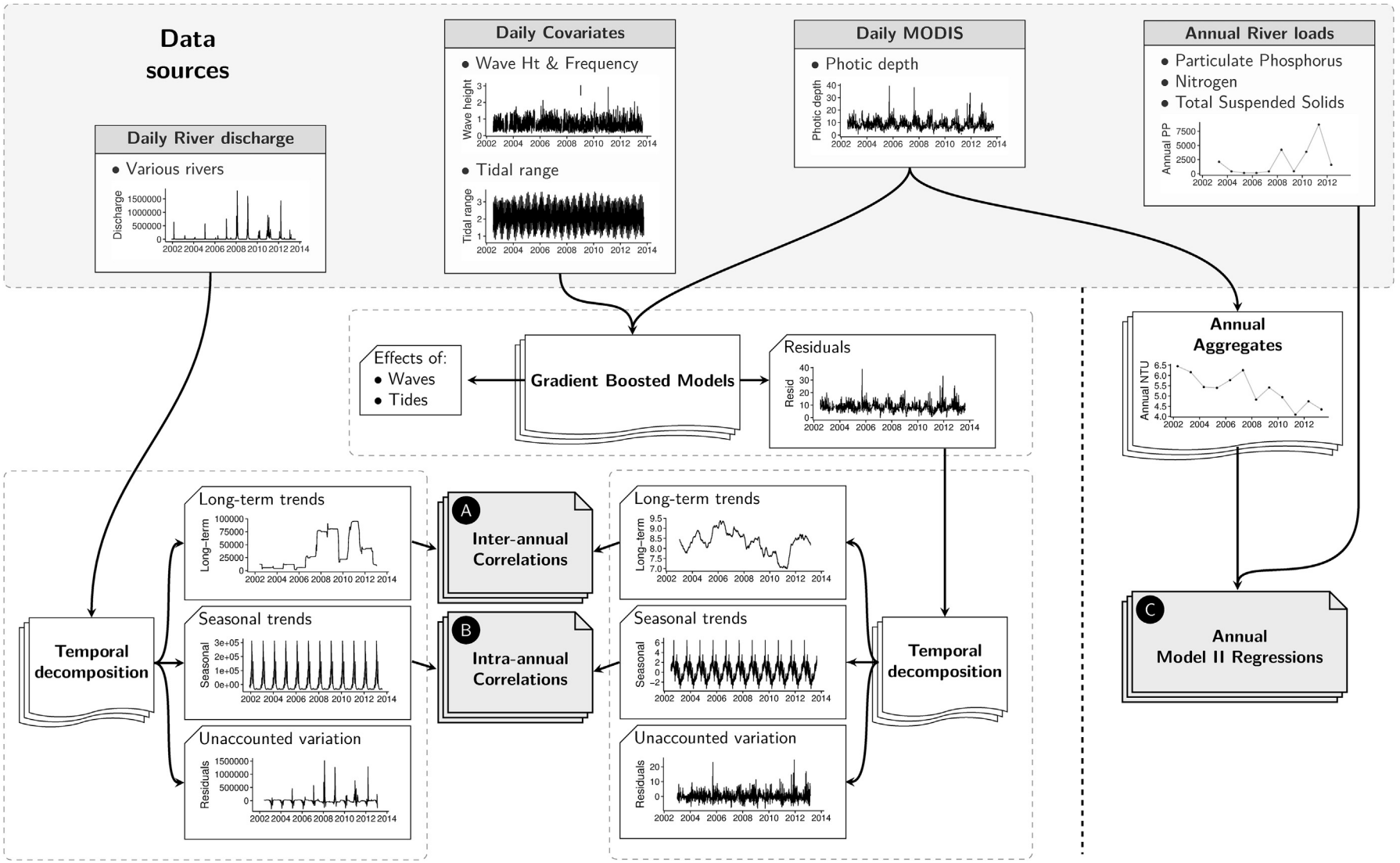

Fig. 2. Flow chart of the individual steps taken in the statistical analyses assessing inter-annual and intra-annual (seasonal) correlations between daily photic depth and daily river discharge volumes (pathway A and B), and of the relationships between annual mean water clarity and annual river nutrient and sediment loads (pathway C). Examples of the raw data are shown in the top panel (grey), of the residual data after adjustment for waves and tides (central panel), and of the final temporally decomposed long-term trends, seasonal variation, and unaccounted variation for both river flows and photic depths (bottom panel).

The second set of river data comprised estimated annual end-of-river loads of particulate phosphorus (PP), total suspended solids (TSS), particulate nitrogen, dissolved inorganic phosphorus and dissolved inorganic nitrogen. Load data were available only as annual rather than daily estimates, and were obtained from Lewis et al. (2014a) for the main rivers in the Wet Tropics, Burdekin and Mackay-Whitsunday Regions, for the 2001/02 to 2012/13 water years (Table 1). For the Normanby Basins, loads were reconstructed from the Source Catchments modelling outputs (Waters et al., 2014) and up-scaled to total catchment flow (Lewis et al., 2014a). For the Fitzroy Basin, loads were compiled from measured data of Packett et al. (2009), Joo et al. (2012), and Turner et al. (2012, 2013). All these estimates are largely derived from end-of-river annual freshwater volume estimates, with correlation coefficients of annual end-of-river freshwater volumes and annual loads of PP or TSS ranging from 0.81 to 0.99 across catchments. Averaged across years, TSS concentrations ranged from 19 to 329 mg L^{-1} across catchments, and PP constituted 0.10%–0.48% of TSS loads. No load data were available for the Burnett, Endeavour and Stewart Rivers. No data exist on the fine sediment component (<16 μm grain size) of river TSS, which is likely the main causative factor for the loss in photic depth (Fabricius et al., 2014; Bainbridge et al., 2015). Due to the highly correlated nature of the available river load estimates, the correlations to the various annual loads (PP, TSS, etc.) gave virtually identical values. As PP is considered the best available proxy for the fine sediment component of the total suspended solids (Bainbridge et al., 2015), only the relationship of photic depth to PP is shown here.

2.5. Statistical methods

The flow chart in Fig. 2 summarises the main steps taken, which largely follow those detailed in Fabricius et al. (2014). To assess inter-annual and seasonal trends in photic depth, our initial analyses focused on daily data. Identifying trends from raw daily data is difficult, due to (1) the noise in photic depth due to short-term variation in the drivers (wave height, wave frequency, wind speed, tidal amplitudes) leading to sediment resuspension, and (2) potential delays in the response of photic depth to the drivers (waves, wind, tides and river discharges). To investigate the potential for delayed responses in photic depth to the environmental drivers, we calculated weighted and unweighted lags with successively larger temporal shifts for each driver in each zone, and identified the lag that maximised their correlation to photic depth. To statistically remove the effects of the short-term drivers (waves, wind and tides), gradient boosted models were then applied to log-transformed and lagged daily data from each zone (Friedman, 2002). The back-transformed residuals from these analyses were then used for further analyses.

To extract the inter-annual (2002–2013) and seasonal trends (i.e., intra-annual cycles based on 365.25 day cyclicity) in photic depths and daily river discharges, temporal decomposition was used (Kendall and Stuart, 1983). This method applies a smooth trend through a time series, decomposing it into its long-term mean trends, seasonal cyclical re-occurring components, and remaining variability. Temporal decomposition was chosen as it does not tend to oversmooth with the same severity as other methods. Since this method cannot incorporate covariates, it was applied to the residuals of the gradient boosted models. Following temporal decomposition, the extracted long-term trends and seasonal cycles were re-centred around the mean observed values for each zone. Correlation analyses were then used to identify the links between detrended daily photic depths and detrended and lagged daily river freshwater discharge volumes. The first set of analyses correlated the long-term detrended (seasonal variation removed) daily values of photic depth with the river discharges (Fig. 2: Pathway A). The second set of analyses correlated the seasonally detrended (long-term trend removed) daily values of photic depth with the river discharges (Fig. 2: Pathway B). To further explore the relationships between the photic depth and river flow time series, covariances were calculated along 100 day running windows of the lagged data. Such covariances quantify associated changes between two time series, and were used to highlight and help understand the links between the trends in river flow and photic depth.

As an independent test of the potential causal relationships between river loads and loss in photic depth, our third set of analyses focused on the annual mean values of photic depth and end-of-river load estimates of particulate phosphorus, other nutrients, and total suspended solids (Fig. 2: Pathway C). These data were not adjusted for the effects of waves, wind and tides, not lagged and not temporally decomposed. The daily data of photic depth were averaged for each 'water year' (1st October to 30th September, i.e., from the start of the wet season to the end of the dry season). The annual loads of PP, TSS and other nutrients were summed across the rivers within each region (Table 1). To account for the uncertainty in river load estimates, Ranged Major Axis regression analysis (Legendre and Legendre, 1998) was used to assess how annual mean photic depth of each zone changed conditional on changes in the annual nutrients and sediment loads. All statistical analyses were done with the statistical software R 3.2.2 (R Development Core Team, 2015).

3. Results

3.1. Spatial patterns and long-term trends in daily photic depth and river freshwater volumes

Long-term mean values of photic depth strongly differed between regions and zones (Fig. 3, Supplementary Table S2). In all regions, mean photic depth increased monotonically from the chronically turbid coastal zones (range: 3.6–4.0 m) to the lagoonal zones. In the three northern regions, mean photic depth continued to increase monotonically to the outershelf zones, whereas in the central and southern regions the differences between lagoonal, mid- and outershelf zones were only minor. Mean photic depths in the outershelf zones ranged from 10.3 m in the Pompey to 14.8 m in the Burdekin Region.

Spatial differences in the long-term mean values of the environmental drivers were strong for tides and river flows, and moderate for waves and wind, reflecting the spatial complexity of the GBR (Supplementary Table S2). Mean daily tidal ranges varied up to 3-fold between zones (range: 1.6 m in the Cape York Outershelf, to 4.8 m in the Broad Sound Inshore zone), and river freshwater discharges varied >5-fold between regions. Mean wave height was ~40% lower in the northern than in the southern GBR (0.50 m *vs.* 0.85 m), and mean wind speed increased ~40% from north to south (from 16 to 23 km h^{-1}).

Temporal dynamics in daily means of wave height (range = 0–3.3 m), wind speed (0–122 m s^{-1}) and tidal ranges (0.3–7.1 m) were stronger than spatial differences in long-term mean values. The analyses of the cross-correlational lags showed that lags of 0 days to waves and tides returned the best model fits, i.e., photic depth was affected more or less instantaneously by waves and tides, and responses to these factors lasted only for a few days. For wind in Cape York, a 5-day lag (the mean wind speed of that day and the four previous days) marginally outperformed the other lags. These lags were included into the final model when statistically removing the effects of waves, wind and tides. In contrast, lags between photic depth and the rivers (rainfall for Cape York) were typically much longer, ranging from 0 days in some

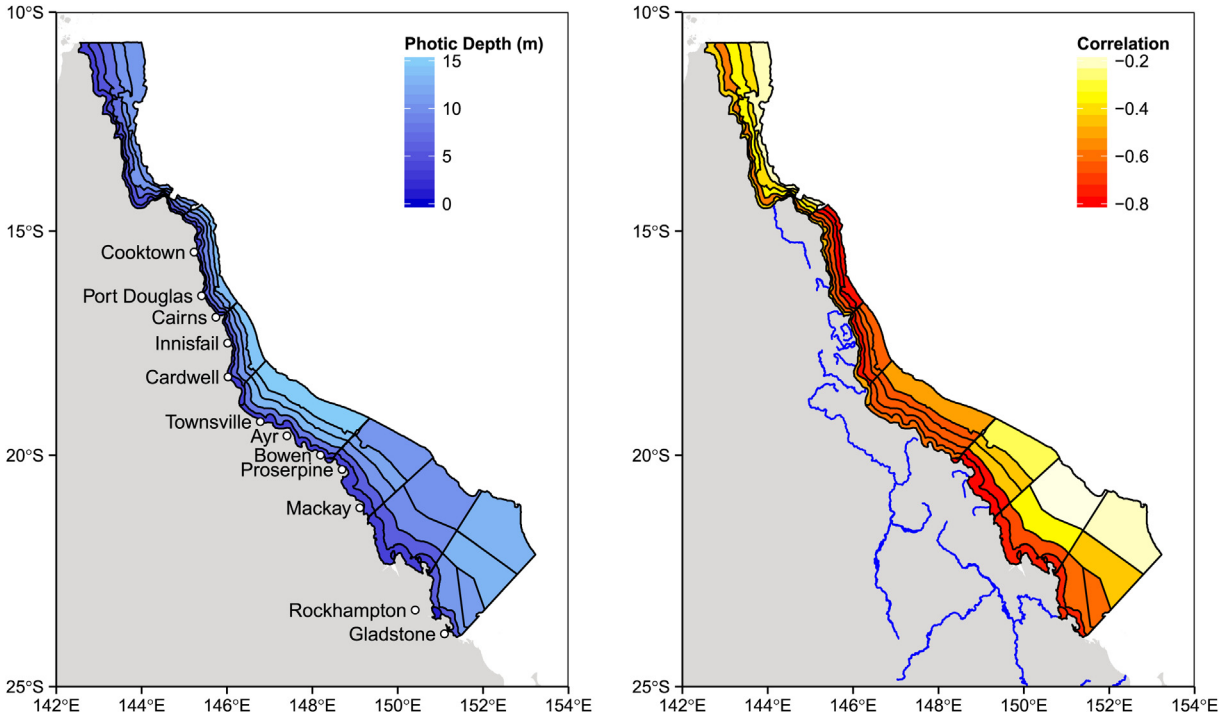

Fig. 3. Left panel: Map of the long-term (11 years) mean photic depth for each zone in the Great Barrier Reef. Right panel: Correlation coefficients, *r*, between daily photic depth (seasonally detrended, and adjustment for waves and tides) and daily river freshwater discharge volumes. The main rivers are mapped as blue lines. For the northern-most region (Cape York) where few river data were available, rainfall data were used as proxy for river discharges.

coastal zones to >180 days in some outershelf zones. These lags were significantly shorter in zones near the rivers *vs.* away from rivers (Fig. 4a, Table 2), reflective of hydrodynamic dispersal. The lags were only marginally related to the extent of catchment modification from where the rivers discharged (Fig. 4a, Table 2).

To quantify the strength of the relationships between photic depth and rivers in the different zones, the daily photic depths data (standardised by the environmental factors and detrended) were related to the daily detrended and lagged river freshwater discharge volumes. The correlations between changes in daily photic depth and river flow were all negative, but the strength of correlations varied widely across zones, ranging from $r = -0.18$ to -0.80 (Figs. 3 and 4b, Supplementary Table S2). Periods of lowest photic depths frequently coincided with the times of highest river flows and *vice versa*, with times of change often coinciding between both data sets (Fig. 5). The correlations were strongest ($r \leq -0.75$) in zones close to river influences (e.g., the Whitsunday Coastal and Inshore zones, and the Southern and Northern Wet Tropic zones), and weakest in the zones away from river influences modification (Fig. 4b, Table 2). The correlations were also stronger in regions with highly modified catchments compared to those with low levels of catchment modification (Fig. 4b, Table 2).

There were substantial differences in the long-term trends of photic depth between the regions and zones. In the three northern regions, periods of steep declines in photic depth alternated with periods of steep recovery, without consistent long-term trends, and there was no obvious classification into wetter and drier periods (Fig. 5, Supplementary Figs. S2, S3). Patterns were particularly pronounced in the Northern and Southern Wet Tropics. Here, the correlation coefficients between photic depth and river flows ranged from $r = -0.63$ to -0.80, except for their chronically turbid coastal zones where values were lower ($r = -0.45$ and -0.50) (Figs. 3 and 5). Changes between the maximum and minimum detrended photic depths were typically ~30%, while detrended river flows varied 7-fold. In these regions, models with no or very short time lags between river flows and photic depth yielded the best model fits (Supplementary Fig. S2), reflecting the narrowness of the continental shelf. 'Spikes' in the covariance between photic depth and discharges were consistently negative, suggesting some rapid impacts yet slow recoveries across the shelf (Fig. 5). There were no lasting signals from the severe Tropical Cyclones Larry (in 2006) and Yasi (2011); the latter possibly masked by the extreme river discharges in this very wet year (Fig. 5).

The remote and sparsely populated Cape York with its minor catchment modifications showed the smallest long-term variation in photic depths (<12%), although river flows varied >12-fold between years ($1.3–16.7 \times 10^6$ ML yr^{-1}). For example, the variation in photic depth between years was <1.5 m in Cape York *vs.* ~2.5 m in the Wet Tropics for Lagoon to Outershelf zones, and <0.5 m *vs.* 1–1.5 m for the Inshore zones. The variations were similar in both regions (~0.5 m) only in the coastal zones. In Cape York, the correlations between photic depth and river flows did not decay systematically across the shelf, and most lags were uninformative, i.e., low photic depth preceded high river flows (Supplementary Fig. S2). In that region, both negative and some positive spikes occurred across the shelf, indicating some sudden declines and relatively rapid recoveries in photic depth. Its photic depth showed a large drop that coincided with severe Tropical Cyclone Monica in 2006, while Tropical Cyclone Ingrid in 2005 did not leave lasting signals.

In the central region and the three southern regions, a period of relative dry years (2002–2006) was followed by periods with high river flows (2007–2013). Many of their inner zones displayed substantial and consistent downward trends in photic depth throughout the 11-year observation period; such downward trends were not apparent in their outer zones or in the northern regions (Fig. 5, Supplementary Figs. S2, S3). In the Burdekin Region, the difference between minimum and maximum detrended photic

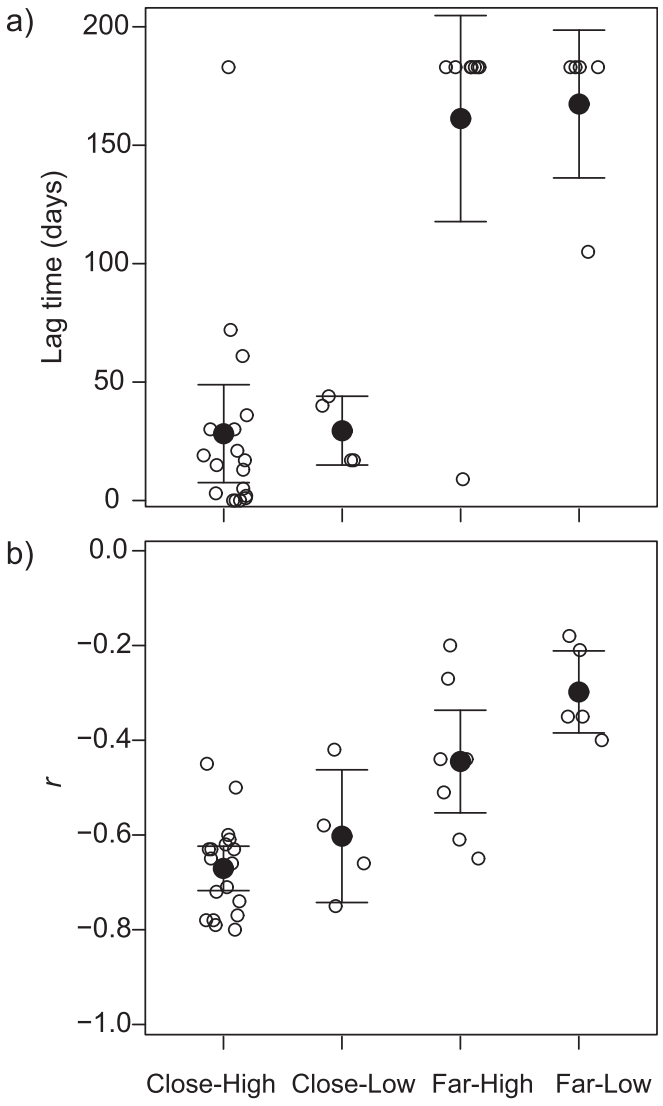

Fig. 4. The effects of distance to rivers (close *vs*. far) and the extent of catchment modification (low *vs*. high; Supplementary Table S2), on (a) optimum correlational lags between daily photic depth and river discharge data, and (b), correlation coefficients, *r*, between daily photic depth versus daily river discharge volumes (after temporal decomposition, i.e., the removal of seasonal trends). Black symbols represent group means, open symbols represent the individual zones, error bars show 1 standard error.

depth was 20–30%, while detrended river flow varied up to 20–fold between years. Negative spikes were pronounced in all zones except the Outershelf, indicating rapid changes in photic depth with changing river flows. The 11 years of data from the Burdekin Region exhibited stronger correlations between river flows and photic depth ($r = -0.51$ to -0.65; Supplementary Fig. S2, Table S2) than previously shown for a 10-year data set (Fabricius et al., 2014), especially for the Mid- and Outershelf zones.

In all southern regions, correlations between river flows and daily photic depth weakened systematically from the inner zones ($r = -0.61$ to -0.79) to the outershelf ($r = -0.18$ to -0.27), likely reflecting the width of the continental shelf (Fig. 3, Supplementary Fig. S3, Table S2). Importantly, photic depth declined consistently throughout the 11-year observation period in most southern inner zones, but not offshore (Fig. 5, Supplementary Fig. S3). The Whitsunday inner zones had the highest correlations of all southern zones, and lags were short, yet they did not show substantial spike. In the Fitzroy Region, the correlations deteriorated from $r = -0.74$ in the Coastal zone to $r = -0.20$ offshore. Inshore, lags were $\leq$13 days, and rapid losses in photic depth were linked to rapid increases in river flows. Correlations in the Broad Sound inner zones were also surprisingly high, despite their distance from the Fitzroy River and the high tidal ranges, however the lags to that river were 36–44 days, and spikes were weak. In the outer zones, photic depth showed one large drop that coincided with massive resuspension events caused by Tropical Cyclone Hamish in 2009 (Fig. 5). This drop was less, yet still detectable, in the midshelf and lagoon zones of this region.

3.2. Seasonal variation in daily photic depth and river freshwater volumes

In many inner zones, photic depth was reduced for many months after rivers started flowing (Fig. 6, Table 3). This was shown by the analyses of seasonal variations in daily photic depth and river flows, after removal of the effects of the environmental drivers and the long-term trends. Averaged across years, rivers started flowing in December/January, peaked in March, declined throughout April, and then remained low for the rest of the year. Synchronously, photic depth declined steeply in most zones from December or January onwards, and reached their seasonal minima in March to May. From then on it increased near-monotonically over a period of four to eight months, and typically returned to 95% of its seasonal maxima in August to December (Table 3, Supplementary Fig. S4, Table S3). For example, Fig. 6 shows the seasonal changes in photic depth and river flows for the Inshore and Midshelf zones in the Northern Wet Tropic Region. Both traces show pronounced cyclicity, with photic depths progressively declining from the time when the river flows started in December to January, reaching lowest values in approximately May when river flows subsided, and recovering from there on. Recovery to 95% of maximum values took until late September on the Midshelf, and until mid-December Inshore (Fig. 6).

Differences in the extent of seasonal decline in photic depth between regions and zones were suggestive of differences in the relative strength and duration of the river effects. Across the whole GBR, the seasonal decline in photic depth between dry season maxima and wet season minima averaged 47.3% (range: 26%–64%). In all regions, seasonal declines were greater in the inner compared to the outer zones (Table 3, Supplementary Fig. S4, Table S3). Across

Table 2
Effects of catchment modification (low versus high) and distance to river mouths (close versus far) on (a) the time lags that optimised the correlations between daily photic depth and daily river discharge volumes, and (b) the correlation coefficients, *r*, between these two measures (Fig. 4, Supplementary Figs. S2, S3, Table S2).

	Df	(a) Lag time			(b) Correlation coefficient		
		MS	F	P	MS	F	P
Modification	1	9132	4.377	0.0447	0.1883	13.62	0.0009
Distance	1	140,232	67.22	<0.0001	0.4779	34.56	<0.0001
Modification* Distance	1	38	0.0180	0.894	0.0099	0.7148	0.404
Residuals	31	2086			0.0138		

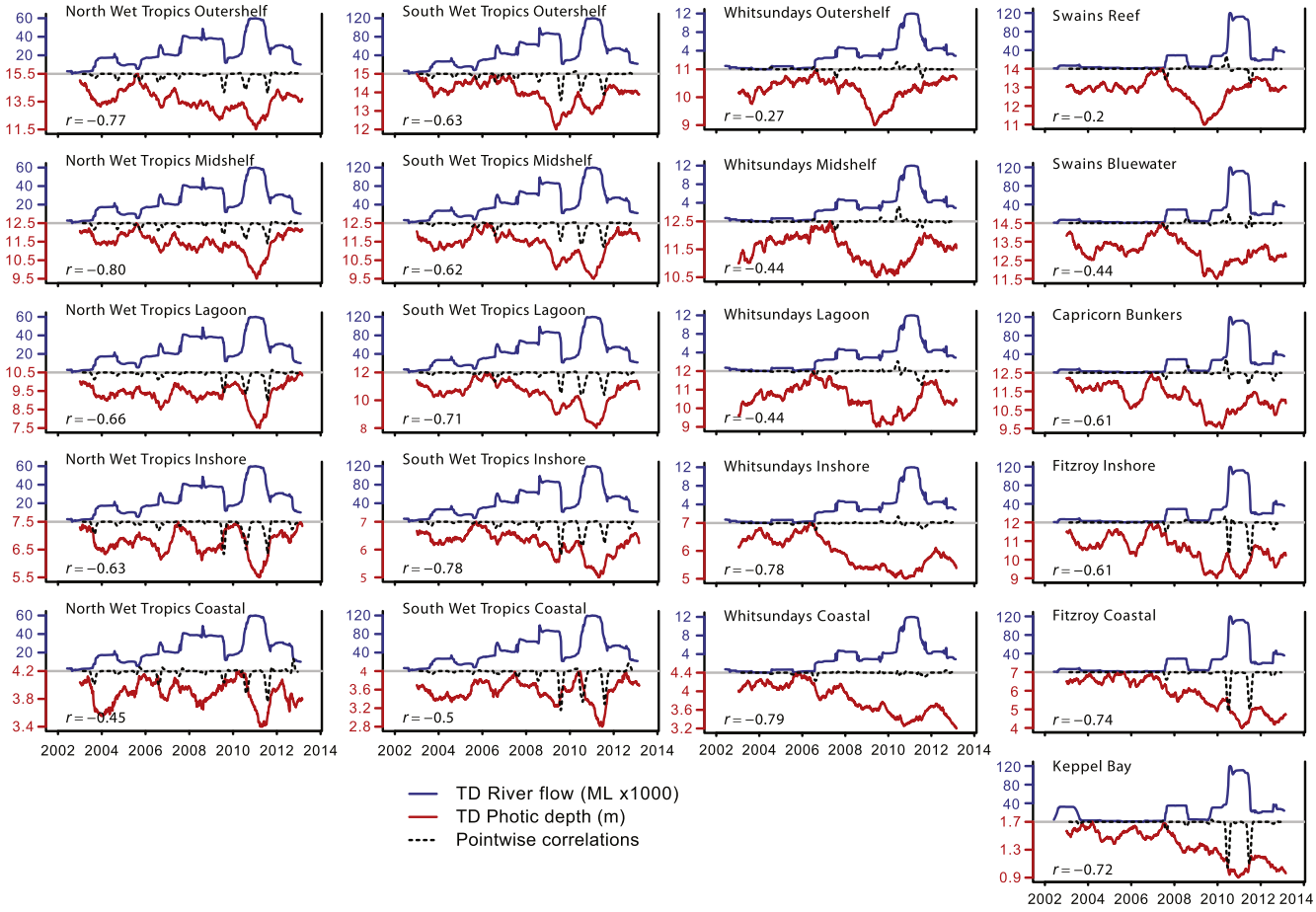

Fig. 5. Long-term trends in river freshwater volumes and photic depth in the Northern and Southern Wet Tropics, Whitsundays and Fitzroy Regions, over 11 years (2002–2013). The blue lines represent the long-term trends in the daily data of river flow, after temporal decomposition (TD, removal of seasonal trends). The red lines represent the long-term trends in the daily data of photic depth, after temporal decomposition and adjustment for waves and tides. The *r* values indicate the strength of the correlations between the two data sets. Black dashed lines represent running covariances between photic depth and discharge/rainfall, highlighting moments (as spikes) when both trends show rapid shifts (negative spikes: changes are in opposite direction, e.g. rapid increase in discharge and decline photic depth; positive spikes: changes are in the same direction). The plots for the other regions are shown in Supplementary Figs. S2 and S3.

regions, the decline was smallest in the Cape York Region (39%, i.e., 3.7 m difference between the seasonal maxima and minima), and greatest in the two Wet Tropic Regions (50%, 6.1 m). Remarkably, in the two Wet Tropic Regions, even the Mid- and Outershelf zones showed a >40% seasonal decline in photic depth, as large as in some inner zones elsewhere (Table 3).

The rates of recovery to 95% of seasonal maxima provided important information about spatial differences in the persistence of the river effects. In all zones, photic depth remained low for several months after river flows subsided (Table 3, Supplementary Fig. S4). The number of days between the seasonal minima in photic depth to 95% recovery varied >2-fold between zones (114–268 days), and averaged 179 days, i.e., 6 months, across the whole GBR (Table 3, Supplementary Fig. S5). Typically, recovery took >200 days in the Coastal and Inshore zones, with the exception of the Fitzroy Region where recovery was faster. Further offshore, recovery often took place in <180 days.

The difference between dry and wet years in the seasonal declines in photic depth and in their rates of recovery also added evidence about the potential role of the rivers in affecting photic depth. In all coastal, inshore, and lagoonal zones of the central and southern regions, seasonal changes in mean photic depth were greater in the wet compared to the dry years (Table 3, Supplementary Fig. S4, S5). Recovery was 10 to >100 days slower in the wet years compared to the dry years (Table 3, Supplementary Table S3).

3.3. Annual mean photic depth and annual river loads

Annual mean photic depth declined with increasing annual river loads of PP in all regions and zones, but declines were particularly pronounced in the inner zones of the most heavily used catchments (Table 3, Supplementary Fig. S5, Table S4). These inner zones (e.g., in the Whitsundays and Fitzroy regions) had >30% lower annual mean photic depth in the years with highest *vs.* lowest PP discharges. In the Northern and Southern Wet Tropics, photic depth was significantly related to river loads all the way across the shelf from the Coastal to the Outershelf zones ($r = -0.65$ to -0.87; Fig. 7, Table 3, Supplementary Table S4). In all zones of these two regions, the annual mean photic depth was 14%–27% lower in the year with highest *vs.* lowest river loads, even including their Mid- and Outershelf zones. Such pronounced differences in photic depth between years with low and high river loads not only reflected the strength of the river effects, but also demonstrated a substantial capacity for recovery of photic depth across years. The relationships between annual mean photic depth and the loads of the other nutrients and TSS (not shown) were almost identical to that of PP.

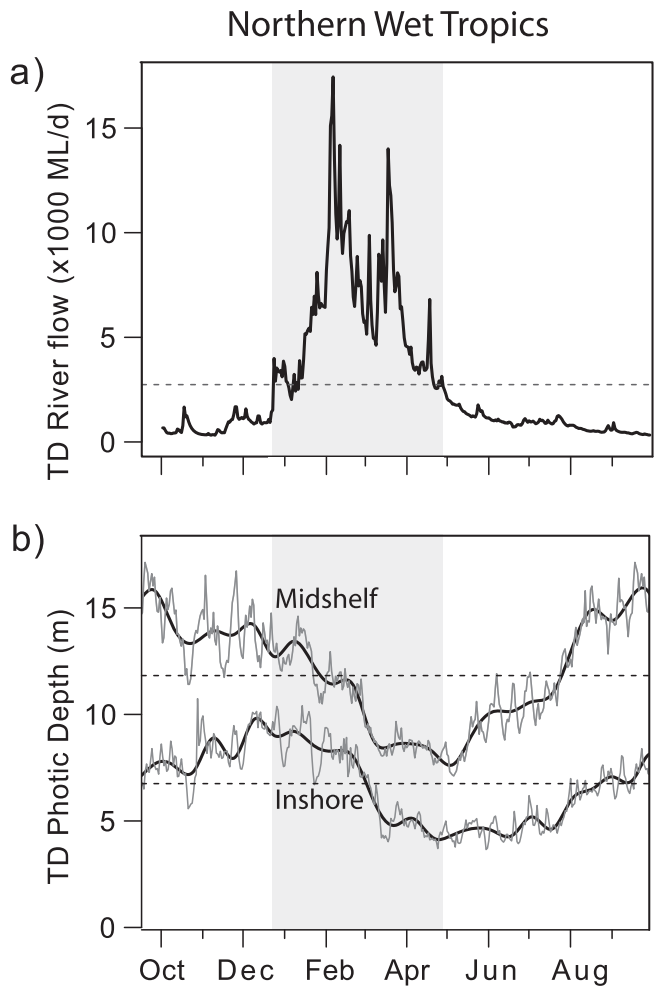

Fig. 6. Seasonal trends of the river discharge volumes summed across all Northern Wet Tropic rivers (a) and photic depth in the Northern Wet Tropics Inshore and Midshelf zones (b). The traces show the seasonal components of the time series after temporal decomposition (removal of long-term trends). The grey fields demarcate times of above-average river flow (January to May). The horizontal dashed lines show the means of photic depths for the Inshore and Midshelf zones. Plots for other regions are shown in Supplementary Fig. S4.

4. Discussion

4.1. Environmental drivers and recovery dynamics of water clarity in shelf seas

This study presents a conceptual and statistical methodology to examine the influence of environmental drivers on marine water clarity. The use of remote sensing data was effective for determining the drivers of GBR water clarity, and particularly suited given the large size and geographic and hydrodynamic complexity of this region. Averaged across the whole GBR, photic depth declined by almost half in response to river discharges, and recovery to 95% of previous maximum values took on average six months. The detection of these changes in these data required controlling for waves and tides, and the separation of long-term trends and seasonal variations. Our analyses showed that reductions in river sediment and nutrient loads will likely result in measurably improved water clarity across much of the GBR on time scale of years rather than decades. The methodology may similarly be used to quantify relationships between water clarity and other natural or anthropogenic drivers such as dredging, storms, ocean circulation patterns, or upwelling. The highly variable and seasonal nature of GBR river flows likely enhanced the detectability of temporal patterns in water clarity, while less variable discharges would likely have caused stronger spatial patterns.

River freshwater volumes and PP load data were used as proxies for the materials that actually cause the loss in photic depth. The annual estimates of the different forms of nutrients, sediments and freshwater were highly correlated within each catchment (Lewis et al., 2014a). For this reason, their individual contributions to the loss in photic depth could not be resolved, and this should be the subject of further study. However, nutrient and sediment loads varied greatly between rivers (Lewis et al., 2014a). The observed losses in water clarity were greatest in the regions with highest river nutrient and sediment loads and intense agricultural land use, namely the Wet Tropic, Whitsunday, Burdekin, and Fitzroy regions (Supplementary Table S1; Kroon et al., 2012; Lewis et al., 2014a). Losses in water clarity were comparatively small in the remote Cape York Region and all offshore zones. Similarly, correlations between river flows and photic depth were strongest in the zones near rivers discharging from modified catchments, where increases in river loads above natural background levels are the greatest (Kroon et al., 2012; Waters et al., 2014). This suggests that fine sediment and nutrient loads are responsible for altered water clarity, and not the freshwater discharges.

Several physical and biological pathways can explain the slow recovery of water clarity in the GBR. First, cycles of resuspension gradually shift the newly imported particulate materials into north-facing bays or deeper waters beyond the reach of storm waves, progressively increasing the amounts of wave and tidal energies required for resuspension (Orpin et al., 2004; Wolanski et al., 2008; Bainbridge et al., 2012; Lewis et al., 2014b). Second, wave action contributes to the compaction and embedding of the newly imported fine materials into existing sea floor sediments, thereby gradually hampering resuspension (Lambrechts et al., 2010). Third, organic flocs are formed as a result of interactions of nutrients with fine sediments, and these flocs initially facilitate resuspension, but eventually break down over time (Bainbridge et al., 2012). Fourth, the gradual depletion of the newly imported nutrients and trace elements leads to a decline in plankton biomass, thereby improving photic depth. Phytoplankton biomass (measured as chlorophyll *a*) declines away from the coast and in winter (Brodie et al., 2007), hence matching the observed changes in photic depth. While phytoplankton contributes far less to declining water clarity in shallow GBR waters than fine sediments, organic flocs, and detritus, its relative contribution can be more significant further offshore (Bainbridge et al., 2012; Macdonald et al., 2013).

In the shallow coastal zones, the relationship between runoff and water clarity was weaker and recovery was slower than in the inshore and lagoonal zones. Thick and predominantly terrigenous sediment wedges are known to cover the seafloor near the river mouths, indicating long-term accumulation of the newly imported fine sediments (Belperio, 1983; Lambrechts et al., 2010). Here, water clarity is chronically lower near than further away from rivers (Fabricius et al., 2013). This indicates that in coastal zones only a proportion of the newly imported resuspendible sediments is being winnowed out each year. Nevertheless, our data show that newly imported materials further reduced coastal water clarity, and that the reductions were greatest in the years with the largest river loads.

4.2. Consequences for ecosystem health and management implications

Prolonged exposure to low photic depth and associated nutrients are known to cause significant water quality related changes in GBR ecosystems. Increased macroalgal cover and bioeroder

Table 3
Seasonal and annual dynamics in values of standardised photic depth for the whole Great Barrier Reef (GBR), and mean values for the 35 zones in the seven regions. (a) Seasonal dynamics: Tabulated are: Seasonal maximum photic depth (PD): the maximum smoothed and standardised photic depth within an annual cycle (Fig. 6, Supplementary Fig S4); Seasonal decline PD: decline between seasonal maximum and minimum photic depth (absolute: in m, and as % of maximum); Seasonal minimum PD Date: date within a year cycle corresponding to the minimum standardised photic depth; Recovery95%: mean number of days between the seasonal minimum PD and the next recovery to 95% of seasonal maximum PD. Seasonal data are estimated separately for dry years (2002–2006) and wet years (2007–2013) in the southern regions. (b) Decline in observed annual mean photic depth (percent, in brackets: lower and upper 95% confidence intervals) between years with maximum vs minimum annual river loads of particulate phosphorus (Fig. 7, Supplementary Fig S6). Confidence interval ranges that do not include zero signify significant differences ($P < 0.05$; in bold).

		(a) Seasonal dynamics						(b) Annual dynamics	
Region	Zone	Dry/wet years	Seasonal maximum PD (m)	Seasonal decline PD (m)	Seasonal decline PD (%)	Seasonal minimum PD (date)	Recovery (Days)	(% decline PD)	(Lower, upper 95% CI)
Mean whole GBR			12.6	5.9	47.3	14 April	179	17.2	(3.9, 30.2)
Cape York	Outershelf	All	13.3	4.8	35.8	26 Jan	233	**13.0**	(3.1, 23.3)
	Midshelf	All	13.5	5.8	43.0	7 Mar	192	6.9	(−4.1, 17.3)
	Lagoon	All	9.2	2.6	28.2	12 Apr	158	**10.7**	(1.4, 19.8)
	Inshore	All	7.0	2.8	40.5	26 Apr	223	**12.5**	(3.4, 21.9)
	Coastal	All	5.2	2.5	48.3	24 Mar	258	**14.3**	(4.4, 24.4)
Northern	Outershelf	All	17.4	7.4	42.8	25 Apr	132	**23.3**	(13.1, 33.3)
Wet	Midshelf	All	15.9	8.3	52.3	3 May	136	**24.2**	(12.5, 35.6)
Tropic	Lagoon	All	12.6	6.6	52.1	29 Apr	148	**26.2**	(13.2, 38.7)
	Inshore	All	9.8	5.6	56.6	25 Apr	225	**22.9**	(14.5, 31.2)
	Coastal	All	6.4	3.8	59.1	18 Jul	197	**14.0**	(4.7, 23.2)
Southern	Outershelf	All	19.4	8.0	41.4	23 Mar	176	**16.8**	(5.5, 27.8)
Wet	Midshelf	All	16.9	7.8	46.4	4 May	131	**21.4**	(5.0, 38.3)
Tropic	Lagoon	All	15.2	7.4	48.9	10 Mar	179	**27.0**	(10.3, 44.3)
	Inshore	All	9.0	4.2	46.8	15 Mar	265	**25.7**	(15.1, 36.9)
	Coastal	All	5.2	2.6	50.5	17 Apr	231	**16.6**	(6.0, 26.9)
Burdekin	Outershelf	Dry	18.6	5.8	31.0	21 Apr	154	8.0	(−0.32, 15.9)
		Wet	19.5	7.7	39.7	16 Mar	182		
	Midshelf	Dry	19.4	9.2	47.5	19 Apr	158	**12.6**	(0.39, 23.7)
		Wet	20.2	10.1	50.2	20 Mar	182		
	Lagoon	Dry	18.3	8.8	48.0	20 Apr	158	**14.7**	(2.1, 26.4)
		Wet	19.9	11.6	58.2	24 Mar	177		
	Inshore	Dry	11.7	5.8	49.1	20 Apr	114	**17.5**	(0.05, 33.3)
		Wet	10.9	6.2	57.2	26 Mar	170		
	Coastal	Dry	4.8	2.0	42.1	21 Apr	228	12.0	(−0.86, 23.9)
		Wet	4.9	2.3	46.9	28 Mar	245		
Whitsunday	Outershelf	Dry	13.2	4.0	30.0	25 Mar	167	7.4	(−4.2, 18.1)
		Wet	13.0	4.3	33.0	03 Apr	158		
	Midshelf	Dry	18.7	10.0	53.6	19 May	137	**11.2**	(0.88, 20.9)
		Wet	17.1	8.6	50.4	22 Mar	183		
	Lagoon	Dry	15.1	7.3	48.1	21 May	122	**18.0**	(3.2, 31.5)
		Wet	15.9	9.2	58.1	22 Mar	179		
	Inshore	Dry	8.6	3.1	36.0	18 Apr	119	**32.6**	(15.1, 50.9)
		Wet	8.1	4.5	56.2	23 Mar	263		
	Coastal	Dry	5.5	2.2	40.7	22 Apr	223	**30.1**	(14.3, 46.1)
		Wet	5.4	2.9	54.1	25 Mar	252		
Broadsound/ Pompey	Pompey	Dry	13.4	5.4	40.0	21 Mar	173	0.78	(−11.4, 12.5)
		Wet	12.4	4.0	32.3	20 Apr	142		
	Lagoon	Dry	13.2	6.4	48.5	06 May	114	7.0	(−7.7, 20.5)
		Wet	14.0	7.7	54.6	21 Mar	189		
	Inshore	Dry	8.0	3.6	44.4	22 Apr	226	**28.0**	(8.9, 46.1)
		Wet	7.6	4.1	54.5	27 Mar	253		
	Coastal	Dry	5.5	3.0	54.7	20 Apr	268	**29.3**	(9.7, 47.9)
		Wet	5.1	3.1	60.1	27 Mar	257		
Fitzroy	Swain Reef	Dry	15.1	4.0	26.4	26 Jun	82	2.6	(−12.9, 16.8)
		Wet	15.8	5.5	34.6	05 Jul	149		
	Swain	Dry	19.9	11.3	56.8	27 May	125	14.0	(−1.4, 30.1)
	Bluewater	Wet	19.1	10.9	57.1	22 May	124		
	Capricorn	Dry	16.9	7.1	42.2	15 May	134	4.7	(−8.4, 16.8)
	Bunker	Wet	16.8	8.4	50.0	16 Mar	186		
	Inshore	Dry	15.7	6.6	42.2	06 Apr	136	8.8	(−2.9, 21.8)
		Wet	17.1	10.1	59.4	12 Mar	185		
	Coastal	Dry	10.1	5.7	57.0	09 Mar	159	**33.6**	(10.5, 56.1)
		Wet	7.9	5.1	64.4	25 Mar	149		
	Keppel Bay	Dry	2.2	1.2	54.1	23 Apr	161	**34.6**	(12.8, 56.0)
		Wet	1.9	1.2	63.1	02 Apr	241		

densities, and reduced coral biodiversity are all strongly related to long-term reductions in water clarity (e.g. De'ath and Fabricius, 2010; Fabricius et al., 2012; Brodie and Waterhouse, 2012). For this reason, water quality guidelines for the GBR are based on annual mean values in water clarity rather than their extreme values (Great Barrier Reef Marine Park Authority, 2009; De'ath and Fabricius, 2010). In other regions such as Hawaii, slow-moving and reworked flood deposits are also assumed to affect benthic communities more than the flood plumes (Storlazzi and Jaffe, 2008). Long-term exposure to low water clarity is often considered even

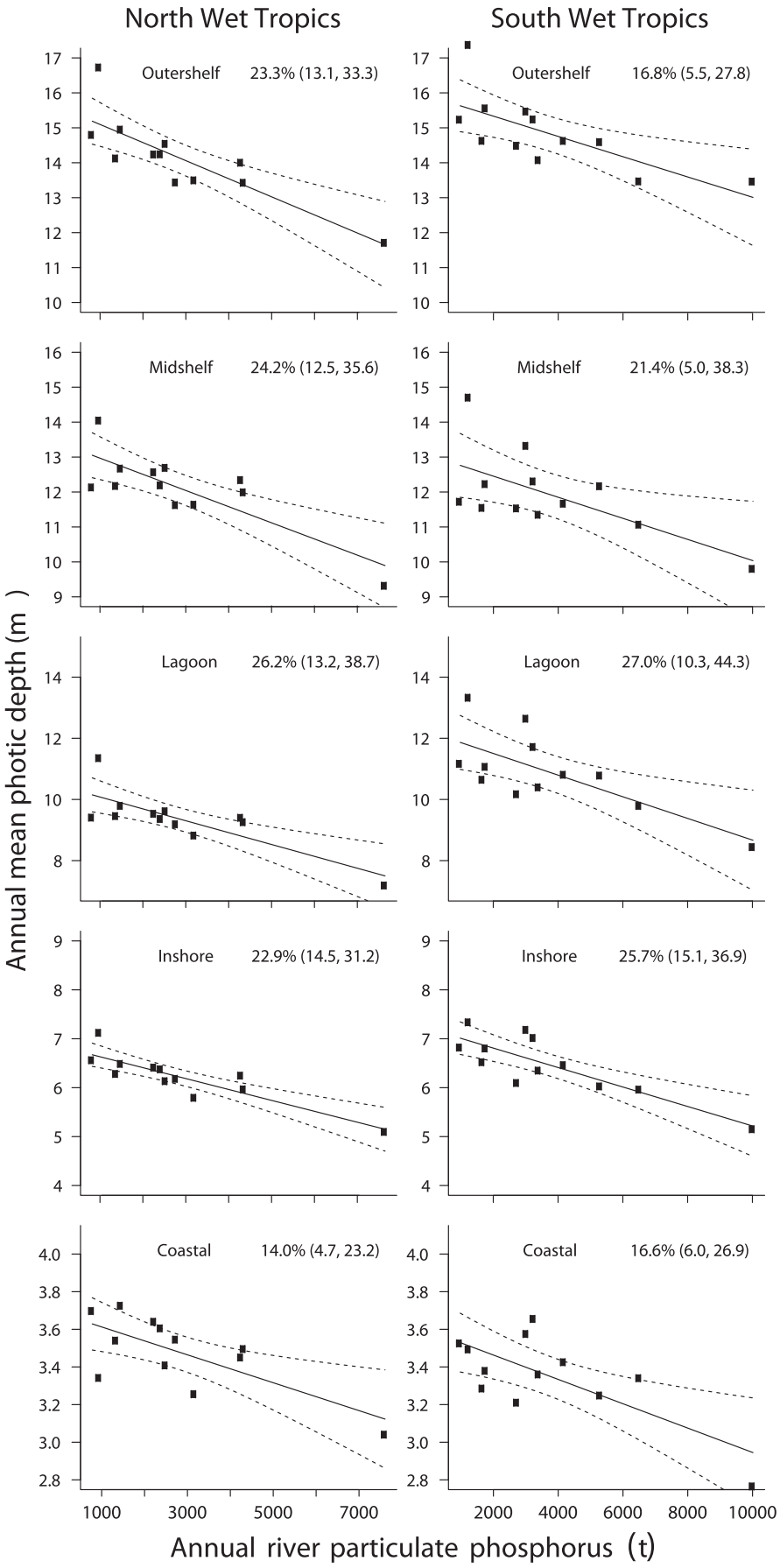

Fig. 7. Relationships between annual mean photic depth and annual river loads of particulate phosphorus in the Northern and Southern Wet Tropical Regions of the GBR (dashed lines: 95% confidence intervals). Note the different scales on both x and y axes. Regression parameters are listed in Supplementary Table S4, plots of other regions are shown in Supplementary Fig. S5.

more influential than the exposure to river plumes (after their salinity has returned to non-stressful levels). Plume sediment, nutrient and pesticide concentrations, and their exposure periods, are typically significantly lower than those that are considered lethal for benthic marine organisms, and resuspension events during storms can lead to higher exposures than those caused by river plumes (Orpin and Ridd, 2012). However, there are examples of additional acute impacts from river plumes, not only through salinity stress. Extensive losses of seagrass meadows in the central GBR in the period 2007–2011 are an example of a relatively acute response to loss of light from decreased water clarity following large Burdekin floods (Petus et al., 2014a). Some macroalgae can also benefit from short-term exposure to dissolved inorganic nutrients, by storing the nutrients in their tissues and thereby promoting growth for the remaining growing season (Schaffelke, 1999).

On the GBR, water clarity is typically highly correlated to the concentrations of chlorophyll, suspended solids, and all forms of particulate nutrients (Fabricius et al., 2005). This correlation suggests another link to ecosystem health. GBR phytoplankton concentrations increase significantly after river floods (Thompson et al., 2014). There is strong evidence for a causative link between higher eukaryotic phytoplankton biomass, higher survival of the larvae of the coral eating starfish *Acanthaster planci*, and subsequent starfish population outbreaks (Brodie et al., 2005; Fabricius et al., 2010). All observed outbreaks originated on mid-shelf reefs within the Northern Wet Tropics Mid- and Outershelf zones, following the largest Burdekin and Wet Tropics river floods on record and coinciding with periods of high reef connectivity (Wooldridge and Brodie, 2015). More work is needed to reliably quantify chlorophyll concentrations from remote sensing data in the optically complex waters of the GBR. Nevertheless, our analyses show for the first time that water clarity in this high-risk region is strongly determined by river nutrient loads, more so than that in other mid- and outershelf zones. These analyses add further evidence to the conclusion that significant reductions in river loads in the Wet Tropic and Burdekin through improved land management may help to reduce the risk of further *A. planci* related coral losses.

Our analyses showed not only large magnitudes and durations of losses in GBR water clarity in response to terrestrial runoff, but also some significant regional differences and long-term trends. The identification of the Wet Tropic as the GBR region that is most severely affected by rivers suggests a potential for management prioritisation of the rivers that had the greatest influence on its water clarity. The study also showed a trend of declining photic depth throughout the 11-year observation period in the central and southern inshore zones, partly due to a combination of high discharges from 2006 to 2011, and incomplete recovery in the years since 2011. The analyses show that reductions in river loads will directly contribute to improving GBR water clarity at management-relevant time scales.

Causal links between land condition, land management and river sediment and nutrient loads have been clearly established (e.g. Kuhnert et al., 2012; Waterhouse et al., 2012; Wilkinson et al., 2013; Bartley et al., 2014, Waters et al., 2014). Coinciding with the expanding agricultural development of the GBR catchments, river sediment and nutrient supplies to the GBR have markedly increased since European settlement (McCulloch et al., 2003; Kroon et al., 2012; Waters et al., 2014). Furthermore, river discharge volumes have also increased after about 1860 due to soil compaction from cattle grazing, and reduced ENSO variance (Lough et al., 2015). Thus, soil and nutrient losses, and river discharge volumes, have been both high in recent decades, with both factors contributing to sediment and nutrient loads. Predicted intensification of rainfall variability due to increasing greenhouse gas concentrations will create further challenges for the retention of nutrients and soils on agricultural lands. This increases the urgency for the wide-spread implementation of more sustainable farming practices, which would likely lead to substantial ecosystem health benefits for the GBR.

Acknowledgements

Many thanks to Ana Rodriguez and Marites Canto for help in processing the remote sensing data, and to the NASA Ocean Biology Processing Group for both the SeaWiFS and MODIS-Aqua satellite-to-*in situ* matchups for the Secchi depth data. Many thanks also to Ivan Valiela, Mike Risk and Glenn De'ath for constructive comments that greatly improved the manuscript. We gratefully acknowledge the following data sources: The State of Queensland's Department of Environment and Heritage Protection provided the wave rider buoy data, the Department of Natural Resources and Mines the daily data of freshwater discharge volumes of the main rivers, the Bureau of Meteorology provided the rainfall and wind data, and the Australian Navy provided the tidal estimates. The study was funded by the Australian Government's National Environmental Research Program – Tropical Ecosystems Hub (NERP Project 4.1), and the Australian Marine Institute of Marine Science.

Appendix A. Supplementary data

Supplementary data related to this article can be found at http://dx.doi.org/10.1016/j.ecss.2016.03.001.

References

Alvarez-Romero, J.G., Devlin, M., da Silva, E.T., Petus, C., Ban, N.C., Pressey, R.L., Kool, J., Roberts, J.J., Cerdeira-Estrada, S., Wenger, A.S., Brodie, J., 2013. A novel approach to model exposure of coastal-marine ecosystems to riverine flood plumes based on remote sensing techniques. J. Environ. Manage 119, 194–207.

Anthony, K.R., Hoegh-Guldberg, O., 2003. Kinetics of photoacclimation in corals. Oecologia 134, 23–31.

Bainbridge, Z., Lewis, S., Smithers, S., Wilkinson, S., Douglas, G., Hillier, S., Brodie, J., 2015. Clay mineral source tracing and characterisation of Burdekin River (NE Australia) and flood plume fine sediment. J. Soils Sediments 16, 687–706.

Bainbridge, Z., Wolanski, E., Lewis, S., Brodie, J., 2012. Fine sediment and nutrient dynamics related to particle size and floc formation in a Burdekin River flood plume, Australia. Mar. Pollut. Bull. 65, 236–248.

Barnes, B.B., Hu, C., Schaeffer, B.A., Lee, Z., Palandro, D.A., Lehrter, J.C., 2013. MODIS-derived spatiotemporal water clarity patterns in optically shallow Florida Keys waters: a new approach to remove bottom contamination. Remote Sens. Environ. 134, 377–391.

Bartley, R., Bainbridge, Z.T., Lewis, S., Kroon, F., Wilkinson, S., Brodie, J., Silburne, D., 2014. Relating sediment impacts on coral reefs towatershed sources, processes and management: a review. Sci. Total Environ 468–469, 1138–1153.

Belperio, A.P., 1983. Terrigenous sedimentation in the central Great barrier reef lagoon: a model from the Burdekin region. BMR J. Aust. Geol. Geophys. 8, 179–190.

Birkeland, C., 1988. Geographic comparisons of coral-reef community processes. In: Choat, J.H., Barnes, D., Borowitzka, M., Coll, J.C., Davies, P.J., Flood, P., Hatcher, B.G., Hopley, D., Hutchings, P.A., Kinsey, D.W., Orme, G.R., Pichon, M., Sale, P.F., Sammarco, P.W., Wallace, C.C., Wilkinson, C., Wolanski, E., Bellwood, O. (Eds.), Proceedings of the 6th International Coral Reef Symposium, Townsville, pp. 211–220.

Brinkman, R., Tonin, H., Furnas, M., Schaffelke, B., Fabricius, K., 2014. Targeted Analysis of the Linkages between River Runoff and Risks for Crown-of-thorns Starfish Outbreaks in the Northern GBR. Terrain Natural Resource Management (NRM), Townsville. http://www.terrain.org.au/Projects/Water-Quality-Improvement-Plan/Studies-and-Reports.

Brodie, J., De'ath, G., Devlin, M., Furnas, M., Wright, M., 2007. Spatial and temporal patterns of near-surface chlorophyll a in the Great Barrier Reef lagoon. Mar. Freshw. Res. 58, 342–353.

Brodie, J., Fabricius, K.E., De'ath, G., Okaji, K., 2005. Are increased nutrient inputs responsible for more outbreaks of crown-of-thorns starfish? an appraisal of the evidence. Mar. Pollut. Bull. 51, 266–278.

Brodie, J., Schroeder, T., Rohde, K., Faithful, J., Masters, B., Dekker, A., Brando, V., Maughan, M., 2010. Dispersal of suspended sediments and nutrients in the Great Barrier Reef lagoon during river-discharge events: conclusions from satellite remote sensing and concurrent flood-plume sampling. Mar. Freshw. Res. 61, 651–664.

Brodie, J., Waterhouse, J., 2012. A critical review of environmental management of the 'not so Great' Barrier Reef. Estuar. Coast. Shelf Sci. 104, 1–22.
Chen, Z., Hu, C., Muller-Karger, F., 2007a. Monitoring turbidity in Tampa Bay using MODIS/Aqua 250-m imagery. Remote Sens. Environ. 109, 207–220.
Chen, Z., Muller-Karger, F.E., Hu, C., 2007b. Remote sensing of water clarity in Tampa Bay. Remote Sens. Environ. 109, 249–259.
Collier, C., Waycott, M., Ospina, A.G., 2012. Responses of four Indo-West Pacific seagrass species to shading. Mar. Pollut. Bull. 65 (65), 342–354.
De'ath, G., Fabricius, K.E., 2010. Water quality as a regional driver of coral biodiversity and macroalgae on the Great Barrier Reef. Ecol. Appl. 20, 840–850.
Devlin, M.J., McKinna, L.C., Alvarez-Romero, J.G., Petus, C., Abott, B., Harkness, P., Brodie, J., 2012. Exposure to riverine plumes in the Great Barrier Reef. Risk assessment by mapping plume extent and composition using remote sensing. Mar. Pollut. Bull. 65, 224–235.
Devlin, M.J., Petus, C., da Silva, E., Tracey, D., Wolff, N.H., Waterhouse, J., Brodie, J., 2015. Water quality and river plume monitoring in the Great barrier reef: an overview of methods based on ocean colour satellite data. Remote Sens. 7, 12909–12941.
Douglas, G., Ford, P., Palmer, M., Noble, R., Packett, R., 2006. Fitzroy River, Queensland, Australia. II. Identification of sources of estuary bottom sediments. Environ. Chem. 3, 377–385.
Fabricius, K., De'ath, G., McCook, L., Turak, E., Williams, D.M., 2005. Changes in algal, coral and fish assemblages along water quality gradients on the inshore Great Barrier Reef. Mar. Pollut. Bull. 51, 384–398.
Fabricius, K., De'ath, G., Humphrey, C., Zagorskis, I., Schaffelke, B., 2013. Intra-annual variation in turbidity in response to terrestrial runoff at near-shore coral reefs of the Great Barrier Reef. Estuar. Coast. Shelf Sci. 116, 57–65.
Fabricius, K., Logan, M., Weeks, S., Brodie, J., 2014. The effects of river run-off on water clarity across the central Great Barrier Reef Mar. Pollut. Bull. 84, 191–200.
Fabricius, K.E., Cooper, T.F., Humphrey, C., Uthicke, S., De'ath, G., Davidson, J., LeGrand, H., Thompson, A., Schaffelke, B., 2012. A bioindicator system for water quality on inshore coral reefs of the Great Barrier Reef. Mar. Pollut. Bull. 65, 320–332.
Fabricius, K.E., Okaji, K., De'ath, G., 2010. Three lines of evidence to link outbreaks of the crown-of-thorns seastar *Acanthaster planci* to the release of larval food limitation. Coral Reefs 29, 593–605.
Friedman, J.H., 2002. Stochastic gradient boosting. Comput. Statistics Data Analysis 38, 367–378.
Gattuso, J.-P., Gentili, B., Duarte, C.M., Kleypas, J.A., Middelburg, J.J., Antoine, D., 2006. Light availability in the coastal ocean: impact on the distribution of benthic photosynthetic organisms and their contribution to primary production. Biogeosciences 3, 489–513.
Great_Barrier_Reef_Marine_Park_Authority, 2009. Water Quality Guidelines for the Great Barrier Reef Marine Park. Great Barrier Reef Marine Park Authority, Townsville.
Hess, S., Wenger, A.S., Ainsworth, T.D., Rummer, J.L., 2015. Exposure of clownfish larvae to suspended sediment levels found on the Great Barrier Reef: impacts on gill structure and microbiome. Sci. Rep. 5, 10561.
Hillier, S., 1995. Erosion, sedimentation and sedimentary origin of clays. In: Velde, B. (Ed.), Origin and Mineralogy of Clays: Clays and the Environment. Springer, Berlin, Heidelberg, pp. 162–219.
IOCCG, 2006. Remote sensing of Inherent Optical Properties: fundamentals, tests of algorithms, and applications. In: Lee, Z. (Ed.), Reports of the International Ocean-colour Coordinating Group, Dartmouth, Canada, p. 126.
Joo, M., Raymond, M., McNeil, V., Huggins, R., Turner, R., Choy, S., 2012. Estimates of sediment and nutrient loads in ten major catchments draining to the Great Barrier Reef during 2006-2009. Mar. Pollut. Bull. Mar. Pollut. Bull.] 65, 150–166.
Kendall, M., Stuart, A., 1983. The Advanced Theory of Statistics. Charles Griffin and Company, London.
Kroon, F.J., Kuhnert, P.M., Henderson, B.L., Wilikinson, S.N., Kinsey-Henderson, A., Brodie, J.E., Turner, R.D.R., 2012. River loads of suspended solids, nitrogen, phosphorus and herbicides delivered to the Great Barrier Reef lagoon. Mar. Pollut. Bull. 65, 167–181.
Kuhnert, P.M., Henderson, B., Lewis, S.E., Bainbridge, Z.T., Wilkinson, S.N., Brodie, J.E., 2012. Quantifying total suspended sediment export from the Burdekin River catchment using the Loads Regression Estimator tool. Water Resour. Res. 48, W04533.
Lambrechts, J., Humphrey, C., McKinna, L., Gourge, O., Fabricius, K.E., Mehta, A.J., Lewis, S., Wolanski, E., 2010. Importance of wave-induced bed liquefaction in the fine sediment budget of Cleveland Bay, Great Barrier Reef. Estuar. Coast. Shelf Sci. 89, 154–162.
Larcombe, P., Ridd, P.V., Prytz, A., Wilson, B., 1995. Factors controlling suspended sediment on inner-shelf coral reefs, Townsville, Australia. Coral Reefs 14, 163–171.
Lee, Z., Darecki, M., Carder, K.L., Davis, C.O., Stramski, D., Rhea, W.J., 2005. Diffuse attenuation coefficient of downwelling irradiance: an evaluation of remote sensing methods. J. Geophys. Res. - Oceans 110, C02017.
Lee, Z., Weidemann, A., Kindlemann, J., Arnone, R., Carder, K.L., Davis, C., 2007. Euphotic zone depth: its derivation and implication to ocean-color remote sensing. Geophys. Res. 112, C3.
Legendre, P., Legendre, L., 1998. Numerical Ecology, second English edition. Elsevier Science BV, Amsterdam.
Lewis, S., Brodie, J., Endo, G., Lough, J., Furnas, M., Bainbridge, Z., 2014a. Synthesizing Historical Land Use Change, Fertiliser and Pesticide Usage and Pollutant Load Data in the Regulated Catchments to Quantify Baseline and Changing Loads Exported to the Great Barrier Reef. Centre for Tropical Water & Aquatic Ecosystem Research (TropWATER), James Cook University, Townsville, Australia, p. 105 pp.
Lewis, S.E., Olley, J., Furuichi, T., Sharma, A., Burton, J., 2014b. Complex sediment deposition history on a wide continental shelf: Implications for the calculation of accumulation rates on the Great Barrier Reef. Earth Planet. Sci. Lett. 393, 146–158.
Lough, J.M., Lewis, S.E., Cantin, N.E., 2015. Freshwater impacts in the central Great barrier reef: 1648–2011. Coral Reefs 34, 739–751. http://dx.doi.org/10.1007/s00338-015-1297-8.
Macdonald, R.K., Ridd, P.V., Whinney, J.C., Larcombe, P., Neil, D.T., 2013. Towards environmental management of water turbidity within open coastal waters of the Great Barrier Reef. Mar. Pollut. Bull. 74, 82–94.
McCulloch, M., Fallon, S., Wyndham, T., Hendy, E., Lough, J., Barnes, D., 2003. Coral record of increased sediment flux to the inner Great Barrier Reef since European settlement. Nature 421, 727–730.
Orpin, A.R., Brunskill, G.J., Zagorskis, I., Woolfe, K.J., 2004. Patterns of mixed siliciclastic–carbonate sedimentation adjacent to a large dry-tropics river on the central Great Barrier Reef shelf, Australia. Aust. J. Earth Sci. 51, 665–683.
Orpin, A.R., Ridd, P., 2012. Exposure of inshore corals to suspended sediments due to wave-resuspension and river plumes in the central Great Barrier Reef: a reappraisal. Cont. Shelf Res. 47, 55–67.
Packett, R., Dougall, C., Rohde, K., Noble, R., 2009. Agricultural lands are hot-spots for annual runoff polluting the southern Great Barrier Reef lagoon. Mar. Pollut. Bull. 58, 976–986.
Petus, C., Collier, C., Devlin, M., Rasheed, M., McKenna, S., 2014a. Using MODIS data for understanding changes in seagrass meadow health: a case study in the Great Barrier Reef (Australia). Mar. Environ. Res. 98, 68–85.
Petus, C., Marieu, V., Novoa, S., Chust, G., Bruneau, N., Froidefond, J.M., 2014b. Monitoring spatio-temporal variability of the Adour River turbid plume (Bay of Biscay, France) with MODIS 250-m imagery. Cont. Shelf Res. 30, 379–392.
Piniak, G.A., Storlazzi, C.D., 2008. Diurnal variability in turbidity and coral fluorescence on a fringing reef flat: southern Molokai, Hawaii. Estuar. Coast. Shelf Sci. 77, 56–64.
Queensland, S.o., 2013. Reef Water Quality Protection Plan - Second Report Card. Queensland Government.
R_Development_Core_Team, 2015. R: a Language and Environment for Statistical Computing. R Foundation for Statistical Computing, Vienna, Austria.
Saulquin, B., Hamdi, A., Gohin, F., Populus, J., Mangin, A., D'Andon, O.F., 2013. Estimation of the diffuse attenuation coefficient K-dPAR using MERIS and application to seabed habitat mapping. Remote Sens. Environ. [Remote Sens. Environ.] 128, 224–233.
Schaffelke, B., 1999. Short-term nutrient pulses as tools to assess responses of coral reef macroalgae to enhanced nutrient availability. Mar. Ecol. Prog. Ser. 182, 305–310.
Seers, B.M., Shears, N.T., 2015. Spatio-temporal patterns in coastal turbidity – long-term trends and drivers of variation across an estuarine-open coast gradient. Estuar. Coast. Shelf Sci. 154, 137–151.
Sheridan, S.C., Pirhalla, D.P., Lee, C.C., Ransibrahmanakul, V., 2013. Evaluating linkages of weather patterns and water quality responses in South Florida using a synoptic climatological approach. J. Appl. Meteorol. Climatol. 52, 425–438.
Storlazzi, C.D., Field, M.E., Bothner, M.H., Presto, M.K., Draut, A.E., 2009. Sedimentation processes in a coral reef embayment: Hanalei Bay, Kauai. Mar. Geol. 264, 140–151.
Storlazzi, C.D., Jaffe, B.E., 2008. The relative contribution of processes driving variability in flow, shear, and turbidity over a fringing coral reef: West Maui, Hawaii. Estuar. Coast. Shelf Sci. 77, 549–564.
Storlazzi, C.D., Norris, B.K., Rosenberger, K.J., 2015. The influence of grain size, grain color, and suspended-sediment concentration on light attenuation: Why fine-grained terrestrial sediment is bad for coral reef ecosystems. Coral Reefs 34, 967–975.
Thompson, A., Schroeder, T., Brando, V.E., Schaffelke, B., 2014. Coral community responses to declining water quality: Whitsunday Islands, Great barrier reef, Australia. Coral Reefs 33, 923–938.
Turner, R., Huggins, R., Wallace, R., Smith, R., Vardy, S., W.M.S, J., 2012. Sediment, nutrient and pesticide loads: Great barrier reef catchment loads monitoring 2009-2010. In: Great Barrier Reef Catchment Loads Monitoring Program. Department of Science, Information Technology, Innovation and the Arts, Brisbane.
Turner, R., Huggins, R., Wallace, R., Smith, R., Vardy, S., W, M. StJ., 2013. Loads of sediment, nutrients and pesticides discharged from high priority Queensland rivers in 2010-2011. In: Great Barrier Reef Catchment Loads Monitoring Program. Department of Science, Information Technology, Innovation and the Arts, Brisbane.
van Maren, D.S., Liew, S.C., Hasan, G.M.J., 2014. The role of terrestrial sediment on turbidity near Singapore's coral reefs. Cont. Shelf Res. 76, 75–88.
Waterhouse, J., Brodie, J., Lewis, S., Mitchell, A., 2012. Quantifying the sources of pollutants in the Great Barrier Reef catchments and the relative risk to reef ecosystems. Mar. Pollut. Bull. 65, 394–406.
Waters, D.K., Carroll, C., Ellis, R., Hateley, L., McCloskey, G.L., Packett, R., Dougall, C., Fentie, B., 2014. Technical Report. Modelling Reductions of Pollutant Loads Due to Improved Management Practices in the Great Barrier Reef Catchments – Whole of GBR, vol. 1. Queensland Department of Natural Resources and Mines, Toowoomba, Australia.
Weeks, S., Werdell, P.J., Schaffelke, B., Canto, M., Lee, Z., Wilding, J.G., Feldman, G.C.,

2012. Satellite-derived photic depth on the Great Barrier Reef: spatio-temporal patterns of water clarity. Remote Sens. 4, 3781–3795.
Wenger, A.S., Johansen, J.L., Jones, G.P., 2011. Suspended sediment impairs habitat choice and chemosensory discrimination in two coral reef fishes. Coral Reefs 30, 879–887.
Wenger, A.S., McCormick, M.I., McLeod, I.M., Jones, G.P., 2013. Suspended sediment alters predator-prey interactions between two coral reef fishes. Coral Reefs 32, 369–374.
Wilkinson, S.N., Hancock, G.J., Bartley, B., Hawdon, A.A., Keen, R., 2013. Using sediment tracing to assess processes and spatial patterns of erosion in grazed rangelands, Burdekin River basin, Australia. Agriculture. Ecosyst. Environ. 180, 90–102.
Wolanski, E., Fabricius, K., Cooper, T., Humphrey, C., 2008. Wet season fine sediment dynamics on the inner shelf of the Great Barrier Reef. Estuar. Coast. Shelf Sci. 77, 755–762.
Wolanski, E., Fabricius, K., Spagnol, S., Brinkman, R., 2005. Fine sediment budget on an inner-shelf coral-fringed island, Great Barrier Reef of Australia. Estuar. Coast. Shelf Sci. 65, 153–158.
Wolanski, E., Marshall, K., Spagnol, S., 2003. Nepheloid layer dynamics in coastal waters of the Great Barrier Reef, Australia. J. Coast. Res. 19, 748–752.
Wooldridge, S., Brodie, J., 2016. Environmental triggers for primary outbreaks of crown-of-thorns starfish on the Great Barrier Reef, Australia. Mar. Pollut. Bull. 101, 805–815.
Zhao, J., Barnes, B., Melo, N., English, D., Lapointe, B., Muller-Karger, F., Schaeffer, B., Hu, C., 2013. Assessment of satellite-derived diffuse attenuation coefficients and euphotic depths in south Florida coastal waters. Remote Sens. Environ. 131, 38–50.